

Analysing Uncertainties in Offshore Wind Farm Power Output using Measure Correlate Predict Methodologies.

Michael Denis Mifsud¹, Tonio Sant², Robert Nicholas Farrugia¹

¹Institute for Sustainable Energy, University of Malta, Marsaxlokk, MXK1351 Malta.

²Department of Mechanical Engineering, University of Malta, Msida, MSD2080, Malta.

Correspondence to: Michael Denis Mifsud (Michael.d.mifsud.10@um.edu.mt)

Keywords: Measure Correlate Predict, Wake Model, Offshore Wind Farms, LiDAR

Abstract

This paper investigates the uncertainties resulting from different Measure-Correlate-Predict methods to project the power and energy yield from a wind farm. The analysis is based on a case study that utilizes short-term data acquired from a LiDAR wind measurement system deployed at a coastal site in the northern part of the island of Malta and long-term measurements from the island's international airport. The wind speed at the candidate site is measured by means of a LiDAR system. The predicted power output for a hypothetical offshore wind farm from the various MCP methodologies is compared to the actual power output obtained directly from the input of LiDAR data to establish which MCP methodology best predicts the power generated.

The power output from the wind farm is predicted by inputting wind speed and direction derived from the different MCP methods into windPRO[®]. The predicted power is compared to the power output generated from the actual wind and direction data by using the Normalised Mean Absolute Error (NMAE) and the Normalised Mean Squared Error (NMSE). This methodology will establish which combination of MCP methodology and wind farm configuration will have the least prediction error.

The best MCP methodology which combines prediction of wind speed and wind direction, together with the topology of the wind farm, is that using Multiple Linear Regression (MLR). However, the study concludes that the other MCP methodologies cannot be discarded as it is always best to compare different combinations of MCP methodologies for wind speed and wind direction, together with different wake models and wind farm topologies.

1 Introduction

The Measure-Correlate-Predict (MCP) methodology introduces uncertainty due to its inherent statistical nature. Recent developments have seen the introduction of new computational regression techniques such as Artificial Neural Networks (ANN) and Machine Learning, which include Decision Trees (DT) and Support Vector Regression (SVR). In a previous study, Light Detection and Ranging (LiDAR) data was used to compare the results of the various regression methodologies at different LiDAR measurement heights (Mifsud, et al., 2018) with the reference site being Malta International Airport (MIA), Luqa, and the candidate site being a coastal watch tower at Qalet Marku on the Northern part of the island. This study uses the same wind data for the year 2016 to construct the MCP models. However, this time the prediction is carried out on both wind speed and wind direction. Wind speed and direction are then predicted for the period June – December 2015. This is done for the different MCP models. The predicted wind speed and wind direction time series are then fed into a wind farm model implemented in windPRO[®] Ver. 2.7 to model the overall energy yield, considering wake losses. The power output for various wind farm configurations is obtained for each methodology. As the LiDAR is sited on the roof of a coastal tower, at a height of 20m above mean sea level, the wind data measured at a height of 80m would be equivalent to a wind turbine (WT) hub height of 100m above the sea surface.

The power output in each case is compared to that obtained when the actual wind data is fed to the wind farm model. Thus, the NMAE, the NMSE and the percentage error in the overall energy yield are

¹ <https://www.emd.dk/windpro>.

46 compared for the various methodologies and wind farm topologies. This is therefore a study about the
47 uncertainties introduced by the various statistical methods, which is then further complicated by the
48 windfarm layout. It is innovative due to the use of an MCP methodology to predict both the wind speed
49 and the wind direction. The following literature review describes different MCP methodologies, four of
50 which are then used in the prediction of wind speed and wind direction. The wake models are also
51 described. This is followed by a description of the methodology used in the study, together with a
52 description of the hypothetical wind farm used as a basis for this study. Finally, the results are presented
53 and discussed.

54 **2. Literature Review**

55 The first MCP methods estimated the mean long-term annual wind speed (Carta, et al., 2013). MCP
56 methods later made use of Simple Linear Regression (SLR) (Rogers, et al., 2005) to establish a
57 relationship between hourly wind characteristics of the candidate and the reference sites. A Multiple
58 Linear Regression is a regression model that involves more than one regressor variable (Montgomery,
59 et al., 2006). The regression is carried out using concurrent wind speed and wind direction data
60 at the reference and the candidate sites. The reference site is normally the closest
61 meteorological station e.g. airports, and the candidate site is the location chosen for the
62 windfarm. When the model is created, hence establishing a relationship between the wind speed
63 at both sites, the long-term wind data at the reference can be used to predict the long-term wind
64 speed at the candidate site. More recent models established non-linear type relationships (Clive, 2004;
65 Carta & Velazquez, 2011) by employing statistical learning (Hastie, et al., 2009). Amongst these are
66 algorithms such as Artificial Neural Networks (ANNs) (Bilgili, et al., 2007; Monfared, et al., 2009) and
67 the more recent Machine Learning (ML) techniques, which include Support Vector Regression (SVR)
68 (Oztopal, 2006; Zhao, et al., 2010; Scholkopf & Smola, 2002; Alpaydin, 2010) and Decision Trees
69 (DTs) (James, et al., 2015; Alpaydin, 2010).

70 A study (Carta, et al., 2013) reviewed many MCP methodologies. These included the method of ratios,
71 first-order linear regression, higher than first-order linear methods, non-linear methods and probabilistic
72 methods. The authors were also concerned with the uncertainties associated with MCP methodologies
73 and argued that users of MCP methodologies have little information on which to determine the
74 uncertainty of the methodology. One methodology to measure this uncertainty is to use the full set of
75 data from the concurrent period to train the model and assess its quality.

76 Another study by Rogers compared four different MCP methodologies (Rogers, et al., 2005). These
77 included a linear regression model, the distributions of ratios of the wind speeds at the two sites, an
78 SVR model and another method based on the ratio of the standard deviations of the two data sets. The
79 authors concluded that SVR gave the best results. In a different study, the same authors (Rogers, et al.,
80 2005b) also analysed the uncertainties introduced with the use of MCP techniques. They concluded that
81 linear regression methodologies could seriously underestimate uncertainties due to serial correlation of
82 data. Another study shows that a proper assessment of uncertainty is critical for judging the feasibility
83 and risk of a potential wind farm development, and the authors describe the risk of oversimplifying and
84 assuming uncertainties (Lackner, et al., 2012).

85 A hybrid MCP method (Zhang, et al., 2014) which involved adding different weights depending on the
86 distance and elevation of the candidate site to the reference sites, was applied to the input of five MCP
87 methodologies. The methods used consisted of the Linear Regression, Variance Ratio, Weibull scale,
88 ANNs and SVR methods. The results were assessed in terms of metrics such as the Mean Squared Error
89 and Mean Absolute Error. Other authors (Perea, et al., 2011) evaluated three methodologies. One
90 method included a linear regression, which was derived from the bivariate normal joint distribution and
91 the Weibull regression method. The other method was based on conditional probability density
92 functions applied to the joint distributions of the reference and the candidate sites. The results from
93 these two methodologies were in turn compared to SVR. Although the conclusion was that the SVR
94 method predicted all the parameters very accurately, the probability density function based on the
95 Weibull distribution was better in terms of prediction accuracy.

96 The ability of ANNs to recognise patterns in complex data sets means that they can also be used to
97 correlate and predict wind speed and wind direction (Zhang, et al., 2014). A neural network contains an
98 input layer, one or more hidden layers of neurons and an output layer. A learning process updates the
99 weights of the interconnections and biases between the neurons in the various layers. The Levenberg-
100 Marquardt (Principe, et al., 2000) algorithm may be used for this purpose. The regression is performed
101 by means of feedforward networks (Alpaydin, 2010) with *multilayer perceptrons* (MLP).

102 Another study (Velazquez, et al., 2011) utilised wind speed and direction from various reference
103 stations. These were introduced into the input layer of an ANN. It was concluded that when wind
104 direction was used as an angular magnitude to the input signal, the model gave better results. Estimation
105 errors also decreased as the number of reference stations was increased. The authors concluded that
106 ANNs are superior to other methods for predicting long-term wind data.

107 The use of ANNs for long-term predictions was also investigated by Bechrakis (Bechrakis, et al., 2004)
108 using wind speed and direction measurements from just one reference station and compared these to
109 standard MCP algorithms. This resulted in an improved prediction accuracy of 5 to 12%. Unfortunately,
110 many models that use various reference stations use only the recorded wind speeds as input. The
111 topologies of the ANNs used have only a single neuron in the input layer, with the output signal being
112 the wind speed at the candidate site (Monfared, et al., 2009; Oztopal, 2006; Bilgili, et al., 2009).

113 Data from meteorological stations possessing long measurement periods provide a large amount of
114 potential inputs for MCP methods. Apart from wind speed and direction, inputs can also include other
115 climatological variables such as air temperature, relative humidity and atmospheric pressure. Hence, a
116 multivariate MCP methodology may be utilised (Patane, et al., 2011). This technique considers all the
117 inputs and extracts the maximum amount of information at the sites. Since some input variables may
118 be inter-correlated, or may not provide information about the target site wind characteristics, the
119 methodology is a two-stage process. Input variables are analysed and those that contain little or
120 redundant information about the candidate site wind characteristics are discarded, following which, a
121 multivariate regression is performed. It was concluded from the results of the tests made that the
122 methodology was more accurate than standard MCP methods, with the quality of the estimation of the
123 long-term wind resource increasing by 19%.

124 SVR is the adaptation of Support Vector Machines to the regression problem. This technique was
125 developed by Vapnik (Vapnik, 1995; Vapnik, et al., 1998) to solve classification problems. SVR
126 (Alpaydin, 2010) is popular within the renewable energy community, being a unique way to construct
127 smooth and nonlinear regression approximations (Diaz, et al., 2017). The analysis of MCP models using
128 SVR techniques shows that SVR is one of the techniques which best represents ML state-of-the-art
129 (Diaz, et al., 2017). This is not only due to its prediction capability, but also to its property of universal
130 approximation to any continuous function, and an efficient and stable algorithm that provides a unique
131 solution to the estimation problem (Diaz, et al., 2017). Different hyperparameters were used to study
132 the SVR methodology. Other studies describe how SVR may be adapted to wind speed prediction
133 (Zhao, et al., 2010).

134 Another recent study shows the importance of DTs in improving the regression results for MCP (Diaz,
135 et al., 2018). The study applied five different MCP techniques to mean hourly wind speed and direction,
136 together with air density, using the data from ten weather stations in the Canary Islands. The study
137 showed that the models using SVR and DTs provided better results than ANNs. A DT is a hierarchical
138 data structure which implements the 'divide and conquer' rule and it may also be applied to the
139 regression problem (Hastie, et al., 2009; Alpaydin, 2010; James, et al., 2015).

140 The use of LiDAR for wind resource assessment (Probst & Cardenas, 2010) shows a distinct advantage
141 of this method over the traditional cup and wind vane measurements. This is demonstrated by studies
142 carried out using different MCP methods such as SLR and ratio analysis. However, no analysis with
143 ANNs, DTs or SVR is carried out. A more recent study (Mifsud, et al., 2018), which utilised the same
144 data as this current study, analysed the accuracy of different MCP methodologies and their capability
145 according to LiDAR measurement height. The study concluded that the MCP accuracy depended on
146 both methodology and measurement height at the candidate site. Other studies using LiDAR at the same

147 measurement site were also carried out. These analysed the turbulent behaviour of the wind data
148 (Cordina, et al., 2017).

149 The issue of wake losses in a wind farm has been described by several authors and can be minimised
150 by optimising the layout of the wind farm (Manwell, et al., 2009). A short literature review of wake
151 models is now presented.

152 Wake models are classified into four categories (Manwell, et al., 2009) which are: Surface roughness
153 models (Bossanyi, et al., 1980), Semi-empirical models (Lissaman & Bates, 1977), (Vermeulen, 1980),
154 Eddy viscosity models (Ainslie, 1985), and Navier-Stokes solutions (Crespo & Hernandez, 1986),
155 (Crespo & Hernandez, 1993). A review of wind turbine wake models (Sanderse, n.d.), shows the effects
156 of reduced power production due to lower incident wind speed and the effect on the wind turbine rotors
157 due to increased turbulence. The author presents a number of reasons on why the focus on numerical
158 simulation is preferred to experimentation; this is mainly due to the use of Computational Fluid
159 Dynamics (CFD). One study presents the mathematical theory behind a simple wake model and that for
160 a multiple wake model (Gonzalez-Longatt, et al., 2012) while another study (Churchfield, 2013)
161 describes a hierarchy of wake models ranging from the empirical to large-eddy simulation (LES). Some
162 of the models compared include Ainslie's Model (Ainslie, 1985), Frandsen's model (Frandsen, 2005),
163 and Jensen's Model (Jensen, 1983). The Dynamic Wake Meandering Model is another method which
164 is described (Larsen, et al., 2008) and also validated (Larsen, et al., 2013) in a study carried out on the
165 Egmond ann Zee offshore wind farm. Another study (Barthelmie, et al., 2006), compares wake model
166 simulations for offshore wind farms, with the wake profiles being measured by Sonic Detection and
167 Ranging (SoDAR). In this case, the models gave a wide range of predictions and it was not possible to
168 identify a model with superior projections with respect to the measurements.

169 In some studies, it is necessary for any wake model used to be straightforward, dependent on relatively
170 few wake measurements and economic in terms of the necessary computing power. Despite their
171 relative simplicity, these models tend to give results which are in reasonable agreement with the
172 available data in the case of a single wake within a small wind farm and a simple meteorological
173 environment. In addition, a comparison of different wake models does not suggest any particular
174 difference in terms of accuracy, between the sophisticated and simplified models (Manwell, et al.,
175 2009).

176 The use of wake models can also be illustrated by considering a semi-empirical model (Katić, et al,
177 1986) that is often used for wind farm output predictions. This model attempts to characterise the energy
178 content in the flow field whilst ignoring the details of the exact nature of the flow field, which is assumed
179 to consist of an expanding wake with uniform velocity deficit that decreases with distance downstream
180 (Manwell, et al., 2009).

181 The N.Ø. Jensen (Jensen, 1983) is a simple wake model based on the assumption of a wake with a linear
182 wake cone. The results from this model are comparable to experimental results.

183 Several metrics may be used to evaluate the accuracy of the models (Rogers, et al., 2005), and it is
184 important to employ more than one metric (Santamaria-Bonfil, et al., 2016) to perform the evaluation.
185 The lower the value of the metric, the better the performance of the model. In this case the Normalised
186 NMAE and the NMSE were used to quantify the performance of the model. The purpose of using
187 normalised values is to provide results which are independent of wind farm sizes (Madsen, et al., 2005).

188 The NMAE is suitable to describe the errors which are uniformly distributed round the mean, revealing
189 also the average variance between the true value and the predicted value (Hu, et al., 2013). The NMAE
190 applies the same weight to the individual errors. The NMSE is a measure of the extent of the dispersion
191 of the errors around the mean and gives a higher weight to larger errors. It assumes that the errors are
192 unbiased and follow a normal distribution (Santamaria-Bonfil, et al., 2016). The percentage error of the
193 energy yield gives an estimate of the accuracy of the model for predicting the total energy generated by
194 the wind farm over the period of evaluation. Due to the fact the each metric has disadvantages that can
195 lead to inaccurate evaluation of the results, it is not recommended to depend only on one measure
196 (Shcherbakov, et al., 2013).

197 **3. Theoretical Background**

198 MCP methods are based on regression techniques. Regression can be performed by using SLR.
 199 However, as mentioned above, several more powerful techniques exist amongst which are ANNs, SVR
 200 and DT. While MCP methodologies have been developed for wind speed, they cannot be directly used
 201 for predicting wind direction (Bosart & Papin, 2017). Nothing has been found in literature on MCP
 202 techniques which explicitly mentions prediction of wind direction at that candidate site. The use of wind
 203 speed vectors is a way of using a regression methodology to predict the wind direction, by breaking the
 204 wind speed vector into its respective components. MCP methodologies are normally used to predict the
 205 wind speed magnitude at the candidate site, but not the direction. Wind velocity may be negative (if
 206 one considers it as a vector) and the MCP methodology normally considers the positive value of the
 207 wind, i.e. magnitude. The methodology used creates a regression model using the wind velocity vector
 208 components to predict the wind vector components at the candidate site (Bosart & Papin, 2017).

209 The methodology is based upon a simple relationship between the meteorological wind direction θ_{met}
 210 and the mathematical wind direction θ_{math} such that:

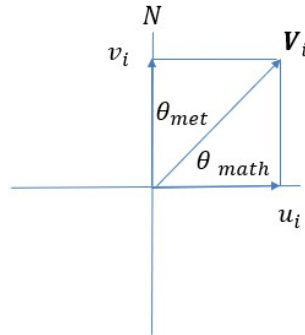
$$\theta_{math} = 90 - \theta_{met} \quad (1)$$

211 in which the wind speed vector V_i can be broken down into its vector components such that

$$u_i = |V_i| \cos \theta_{math} = |V_i| \cos(90 - \theta_{met}) \quad (2)$$

$$v_i = |V_i| \sin \theta_{math} = |V_i| \sin(90 - \theta_{met}) \quad (3)$$

212 in which case the values of u_i and v_i , which may be either positive or negative depending on the
 213 direction of the wind (the value of θ_{met}), are the wind components in the North (y) and the East (x)
 214 directions (axes). The relationship is shown in Figure 1.



215

216 *Figure 1: Difference between the meteorological wind direction and the mathematical wind direction and the component of*
 217 *the wind vector.*

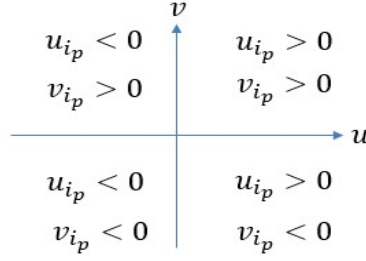
218 Also,

$$|V_i| = (u_i^2 + v_i^2)^{\frac{1}{2}} \quad (4)$$

219 The regression is carried out between the respective components of the wind velocity in the y and x
 220 directions, hence establishing a relationship between the components at both sites. The forecasted wind
 221 direction at the candidate site is then obtained from the forecasted wind components using the
 222 relationship in Eq. (5):

$$\theta_{met_{i_p}} = 90 - \tan^{-1} \frac{v_{i_p}}{u_{i_p}} \quad (5)$$

223 The value of the angle $\theta_{met_{i_p}}$ depends on the direction of u_{i_p} and v_{i_p} , as shown in Figure 2



224

225

Figure 2: Calculating the value of $\theta_{met_{i_p}}$ according to the value of u_{i_p} and v_{i_p} .

226

and in accordance with the relationships shown in Eq. (6):

$$\begin{aligned}
 u_{i_p} > 0 \text{ and } v_{i_p} > 0 \text{ NE winds } & 0^\circ < \theta_{met_{i_p}} < 90^\circ \\
 u_{i_p} > 0 \text{ and } v_{i_p} < 0 \text{ SE winds } & 90^\circ < \theta_{met_{i_p}} < 180^\circ \\
 u_{i_p} < 0 \text{ and } v_{i_p} < 0 \text{ SW winds } & 180^\circ < \theta_{met_{i_p}} < 270^\circ \\
 u_{i_p} < 0 \text{ and } v_{i_p} > 0 \text{ NW winds } & 270^\circ < \theta_{met_{i_p}} < 360^\circ
 \end{aligned} \tag{6}$$

227

and Eq. (7):

$$\begin{aligned}
 u_{i_p} = 0 \text{ and } v_{i_p} > 0 \text{ (North Wind) } & \theta_{met_{i_p}} = 0^\circ \\
 u_{i_p} = 0 \text{ and } v_{i_p} < 0 \text{ (South Wind) } & \theta_{met_{i_p}} = 180^\circ \\
 u_{i_p} > 0 \text{ and } v_{i_p} = 0 \text{ (East Wind) } & \theta_{met_{i_p}} = 90^\circ \\
 u_{i_p} < 0 \text{ and } v_{i_p} = 0 \text{ (West Wind) } & \theta_{met_{i_p}} = 270^\circ
 \end{aligned} \tag{7}$$

228

The results are compared by using the NMAE and the NMSE of the residuals, using the Eq (8) to Eq. (12). The residuals, e_i are the errors between the predicted and the actual output power values from the windfarm,

229

230

$$e_i = P_i - P_{act_i} \tag{8}$$

231

The formula used to calculate the NMAE is shown in Eq (9), whereby the errors are normalised by dividing by the average power production over the whole period of evaluation (Madsen, et al., 2005):

232

233

$$NMAE = \frac{\sum_{i=1}^N |e_i|}{\sum_{i=1}^N P_i} \tag{9}$$

234

And the NMSE is given by:

$$NMSE = \frac{1}{\bar{P} \cdot \overline{P_{act}}} \sum_{i=1}^N (e_i)^2 \tag{10}$$

235

where,

$$\bar{P} = \frac{1}{N} \sum_{i=1}^N P_i \quad (11)$$

236 and

$$\overline{P_{act}} = \frac{1}{N} \sum_{i=1}^N P_{act_i} \quad (12)$$

237 The percentage error in overall energy yield is given by Eq (13), where:

$$e_{eng} = \left(\frac{\sum_{i=1}^N P_i - \sum_{i=1}^N P_{act_i}}{\sum_{i=1}^N P_{act_i}} \right) \cdot 100\% \quad (13)$$

238 4. A Case Study - Site Conditions and the Modelled Offshore Windfarm

239 4.1 The reference and candidate sites

240 The reference site employed in this study is the Meteorological Office at Malta International Airport
 241 (MIA), Luqa, and the candidate site is data collected by a ZephIR 300 LiDAR
 242 (<https://www.zxlidars.com/wind-lidars/zx-300/>, n.d.) unit administered by the University of Malta's
 243 Institute for Sustainable Energy. The unit was situated on the roof of a coastal watch tower at Qalet
 244 Marku, situated in the Northern Part of the Island of Malta (Mifsud, et al., 2018). The relative location
 245 of the two sites is shown in Figure 3, while Figure 4 shows a satellite image of the location of the coastal
 246 watch tower.



247

248 *Figure 3: Map of Malta showing relative location of the candidate and the reference sites (Google,*
 249 *2019) (© Google Maps 2019).*



250

251 *Figure 4: Satellite imagery of the Qalet Marku coastal watch tower, located on a promontory near*
 252 *Bahar ic-Caghaq (Google, 2019) (© Google Maps 2019).*

253 Table 1 and Table 2 show the properties of the candidate and the reference sites respectively (Cordina,
 254 et al., 2017), (Mifsud, et al., 2018). In this case the wind data measured by the LiDAR at a height of
 255 80m, would be equivalent to a cumulative height of 100m above sea-level, which would be the hub
 256 height of the wind turbines in the windfarm. This is because the LiDAR is situated on the rooftop of a
 257 coastal tower at a height of 20m above sea level, as shown in Table 3.

258

Table 1: Candidate Site parameters (Cordina, et al., 2017).

Station Name	Qalet Marku LiDAR Station
LiDAR Type	ZephIR 300 (https://www.zxlidars.com/wind-lidars/zx-300/ , n.d.)
Cone Angle, LiDAR aperture height above the tower rooftop.	60° 1 m
Measurement height, above the LiDAR aperture window, m	80m
Data	Average hourly wind speed, wind direction, atmospheric pressure and relative humidity.
Data range	26 th June, 2015 – 31 st December, 2016
Geographical Coordinates	35.946252°N, 14.45329°E
Average tower rooftop height above surrounding ground level	10 m
Height of base of tower above sea level	6 m

259

Table 2: Reference Site parameters (Malta International Airport).

Station Name	Luqa MIA Weather Station
Measuring Instruments	Wind – Cup and vane Digital temperature probe Digital Barometer.
Data	Average hourly wind speed, wind direction, air temperature, atmospheric pressure and relative humidity.
Mast height	10 m above ground
Height of site above sea level	78 m
Geographical Coordinates	35.85657°N, 14.47676°E

260 4.2 The Available Wind Data

261 The measurement campaign at the candidate site started on the 1st July 2015 and ended on the 31st
 262 December 2016. Hourly wind data were available for this time period from both the reference and
 263 candidate sites. The ideal number of data points used to create the MCP models is thus 8784, i.e. the

264 number of hours in 2016. Following analysis and filtration of the wind speed data at the reference site,
 265 98% of the data was considered as suitable for the creation of the model. The data at the reference site
 266 was all considered as suitable. Hence, the regression model was created using the concurrent 8616 wind
 267 speed and direction values. For the year 2015, 95.6% of the data was considered valid (the measurement
 268 campaign started on the 26th of June, 2015, hence there were 4368 hours of wind speed and direction
 269 measurement of which 4176 were valid data points).

270 The MCP analysis was carried out using both wind speed and wind direction. The data from the
 271 reference site were used as the independent data set. The models were created using the data for the
 272 year 2016, while the reference site wind data for 2015 used to create the predicted wind speed and wind
 273 direction as inputs to the windfarm model.

274 4.3 The Wind Farm Design in windPRO®

275 *Table 3: Wind Turbine Parameters used in the study (wind-turbine-models.com, 2019).*

Wind Turbine Parameter	
Manufacturer	RE Power (Germany)
Rated Power	5000 W
Rotor orientation	Upwind
Number of blades	3
Rotor Diameter	126 m
Swept Area	12469 m ²
Blade Type	LM
Cut in speed	3.5 ms ⁻¹
Rated Wind Speed	14 ms ⁻¹
Cut out speed (for off-shore)	30 ms ⁻¹
Hub-height, z	100 m

276 The hypothetical wind farm is located opposite the coastal watch tower of Qalet Marku [14.452498°E,
 277 35.945892°N]. windPRO® 2.7 was used to render an image of the wind farm onto an image of the
 278 LiDAR unit taken from the watch tower. This gives an indication as to the extent of the wind farm. This
 279 is shown in Figure 5, while Figure 6 shows the satellite imagery of the wind farm, showing a 250-MW
 280 capacity windfarm. The windfarm faces the North-West direction, which is the prevailing wind
 281 direction.

282 The windfarm is made up of 50 wind turbines. There are 10 wind turbines in a row, having a cross-wind
 283 spacing of five rotor diameters (5D). The distance between the successive rows of wind turbines, or the
 284 downwind spacing is eight rotor diameters (8D). Thus, considering wind turbines with a rotor diameter,
 285 D , of 126 m (for a 5 MW Wind Turbine), the distance between the turbines in the cross-wind direction
 286 is 630 m, and the distance between successive rows of wind turbines in the downwind direction is
 287 1,008 m. The wind turbine selected for use in windPRO® is the RE Power 5-MW wind turbine whose
 288 parameters are shown in Table 3.



289
 290 *Figure 5: View of the wind farm rendered onto an image of the area and also showing the LiDAR unit.*



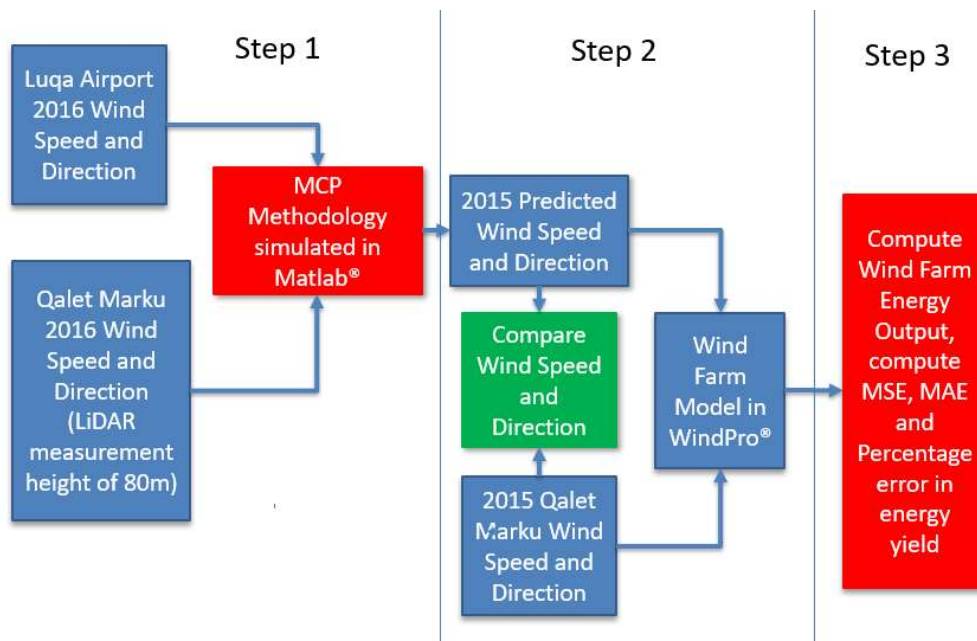
291
292
293

Figure 6: Satellite imagery of the wind farm showing the location of the 50 wind turbines with respect to the coastal LiDAR station (Google, 2019) (© Google Maps 2019).

294 5. Methodology

295 Figure 7 shows the methodology applied in this paper. The study is divided into three steps as follows:

- 296 1. STEP 1 - The various MCP methodologies are used to compute the MCP model. For wind speed,
297 the models are trained using wind speed and direction data at a candidate and reference site for the
298 year 2016. For the wind direction the input training data is the wind velocity vector component in
299 the North or East direction at the candidate site, and the output of the model is the respective
300 component at the candidate site. The models are summarised in Table 4, below. Table 4 describes
301 the inputs used to train the respective models, both for wind speed and wind direction. It also shows
302 the parameters of the models and the algorithms used to train the model, such as Least-Squares for
303 MLR and the Levenberg-Marquardt algorithm for ANN.
- 304 2. STEP 2 - The 2015 wind speed and wind direction are predicted using the models computed in
305 Step 1. The predicted and actual wind speed and wind direction are used to compute the power
306 output from the wind farm. This is done by feeding the wind speed and direction data into the
307 windPRO® model, and,
- 308 3. STEP 3 - compute and compare the MSE, NMAE and percentage error in the power.



309
310

Figure 7: Applied methodology.

311

Table 4: Description of the regression methodologies used for the Measure-Correlate-Predict Methodology.

MCP methodology	Wind Speed	Wind Direction
MLR	Independent variables: 2 (Wind speed magnitude, wind direction at the reference site). Dependent variables: Wind Speed magnitude at candidate site. Methodology: Least Squares	Independent variable: Wind velocity vector in North and East direction at reference site. Dependent variable: Wind velocity vector in North and East direction at candidate site.
ANN	Number of inputs: 2 - Wind speed magnitude, wind direction at the reference site) Number of outputs: 1 - Wind speed magnitude at candidate site. Number of layers: 3 Number of neurons in layer: 30,30,10 Training Methodology: Levenberg-Marquardt Algorithm Percentage of points used for training: 70% Percentage of points used for verification: 15% Percentage of points used for testing: 15%	Number of inputs: 1 - Wind velocity vector in North and East direction at reference site) Number of outputs: 1 - Wind velocity vector in North and East direction at candidate site.
DT	Number of inputs: 2 - wind speed magnitude, wind direction at reference site. Number of outputs: 1 - wind speed at candidate site. Number of Trees: 200 Minimum Number of Leafs: 5 Methodology: Tree Bagger Ensemble	Number of inputs: 1 - Wind velocity vector in North and East direction at reference site. Number of outputs: 1 - Wind velocity vector in North and East direction at candidate site.
SVR	Number of inputs: 2 - wind speed magnitude, wind direction at reference site. Number of outputs: 1 - wind speed magnitude at candidate site. Methodology: Hyperparameter optimisation, Kernel: Gaussian Solver: Sequential Minimal Optimisation	Number of inputs: 1 - Wind velocity vector in North and East direction at reference site. Number of outputs: 1 - Wind velocity vector in North and East direction at candidate site.

312

The combinations of LiDAR measurement heights and MCP methodologies are shown in Table 5.

313

Table 5: Summary of combinations of methodologies, LiDAR measurement heights and amount of wind turbines used in the analysis

314

80m (equivalent to a 100m hub height)	MCP Methodology			
	Simple Linear Regression (SLR)	Artificial Neural Networks (ANN)	Decision Trees (DT)	Support Vector Regression (SVR).
	Wind Speed, Wind Direction, predicted for 2015. Actual and predicted sequences fed into wind farm model, comparisons of wind farm power output made for a capacity of 250, 200, 150, 100 and 50 MW.			

315

Regression models were created for the MCP methodologies using the reference and candidate wind speed and direction for the year 2016. These regression models were created using SLR, ANN, DT and SVR. A model was created for both wind speed and direction.

316

317

318

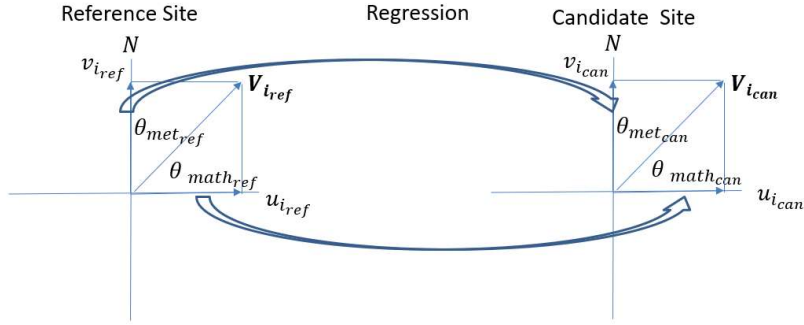
The wind speed and wind direction for 2015 were then predicted with the models by feeding the speed and direction values from the reference site from the year 2015. Thus, a sequence of predicted wind speeds and wind direction time series could be compared to the actual speed and direction measured at the candidate site for the year 2015. The models for the wind speed and the wind direction are independent from each other.

319

320

321

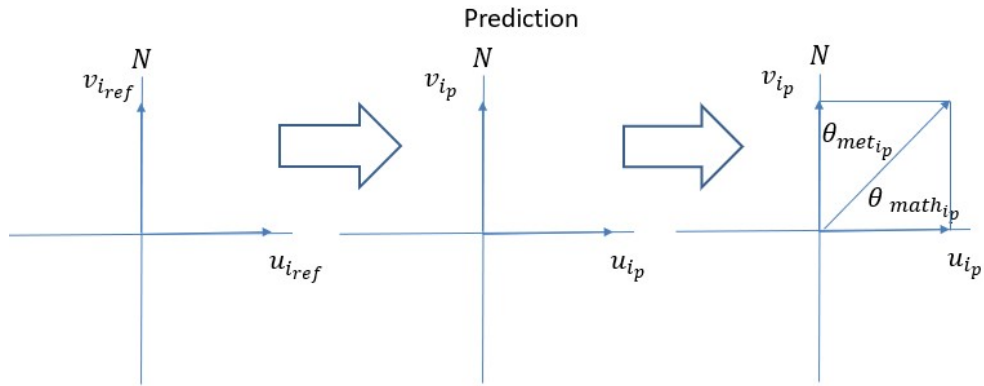
322



323
324

Figure 8: Application of regression methodologies to wind direction

325 In the case of wind direction, the MCP methodologies are applied as shown in Figure 8 and Figure 9.
326 Figure 8 shows that two regressions are carried out: one for the magnitude of the wind component in
327 the North direction and one for the wind component in the East direction. Thus, two models are created
328 using the wind speed and direction data of the reference and the candidate site for 2016. The two models
329 are then used to derive the predicted wind direction for 2015 at the candidate site as shown in Figure 9,
330 by using the wind components at the reference site for 2015 as inputs to the respective models. The
331 values of the wind speed in the North direction and the East direction are first predicted, and the wind
332 direction at the candidate site for 2015, $\theta_{met,p}$, is then derived from the mathematical relationships given
333 in Eq. (6) and Eq. (7).



334
335

Figure 9: Predicting the wind direction

336 The sequences of wind speed and wind directions (both actual and predicted) were fed into the wind
337 farm model. This was done for different combinations of methodology and wind farm (250, 200, 150,
338 100 and 50 MW) configurations. The results were compared to determine which combination of MCP
339 methodology, and windfarm capacity would give the lowest prediction error. The prediction error for
340 the power output from the wind farm is analysed using the Mean Squared Error (MSE), the Normalised
341 Mean Absolute Error (NMAE) and the percentage error in the Overall Energy Yield for the period of
342 analysis. The results are shown in the following section.

343 6. Results

344 A summary of the results is shown below where sequences of data for a specific period of 2015 are
345 compared. These sequences are for wind speed, wind direction and power output. All MSE, NMAE and
346 percentage errors in the overall energy yield are then shown in the following tables.

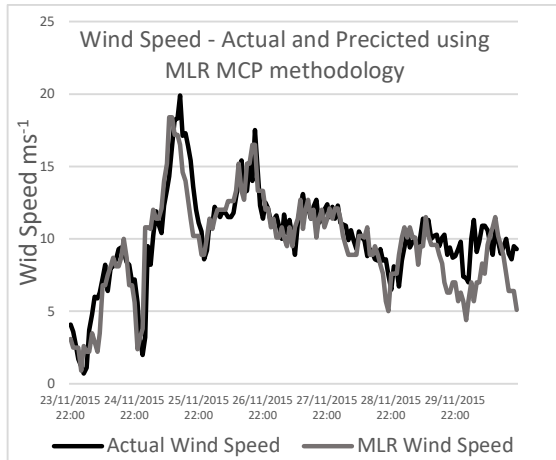
347 6.1 Wind speed and wind direction with MCP methodology.

348 6.1.1 Wind speed with MCP methodology.

349 Figure 10 to Figure 13 show the wind speed from the period 23rd November to the 30th November 2015.
350 The particular period is chosen because of the high availability of wind. The actual wind data are

351 compared with that predicted by the MLR, ANN, DT and SVR methodologies. The predicted wind
 352 values closely follow the actual wind values, for all the MCP methodologies applied.

353



354
 355 *Figure 10: Comparing actual wind speed and wind speed*
 356 *predicted by MLR methodology with wind data for 2015*

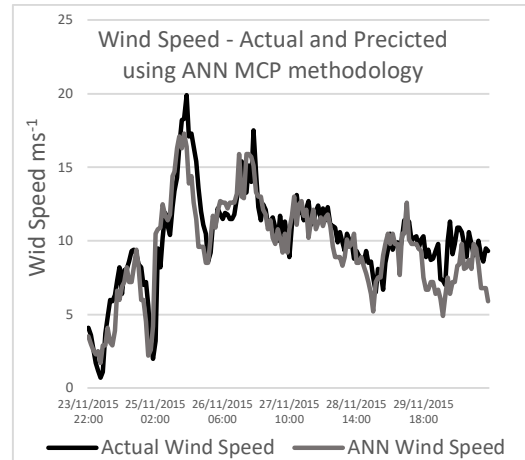
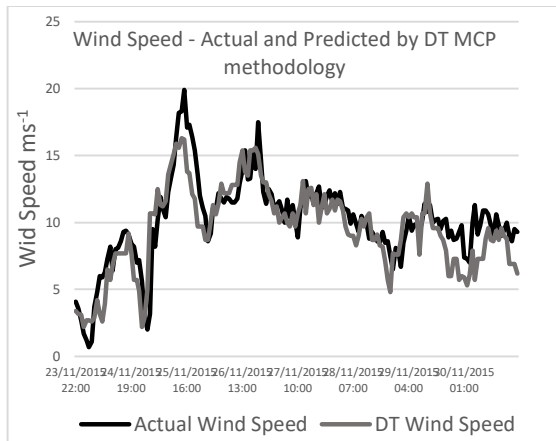


Figure 11: Comparing actual wind speed and wind speed
predicted by ANN methodology with wind data for 2015.



360
 361 *Figure 12: Comparing actual wind speed and wind speed*
 362 *predicted by ANN methodology with wind data for 2015*

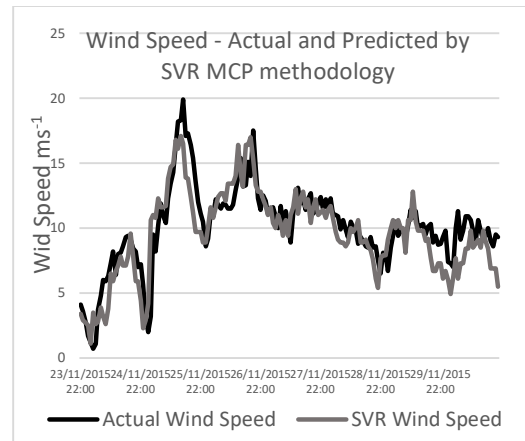
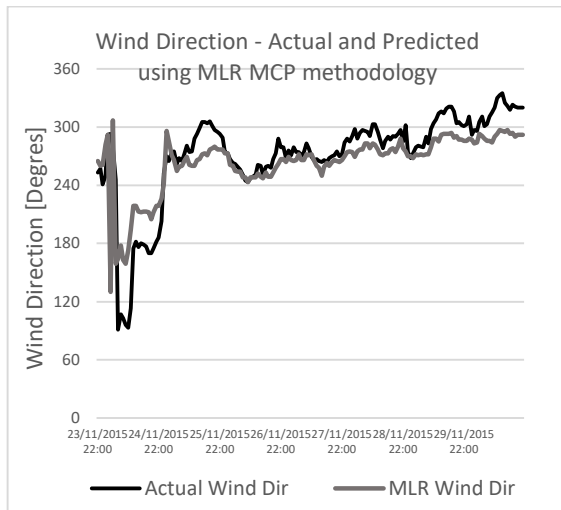


Figure 13: Comparing actual wind speed and wind speed
predicted by SVR methodology with wind data for 2015.

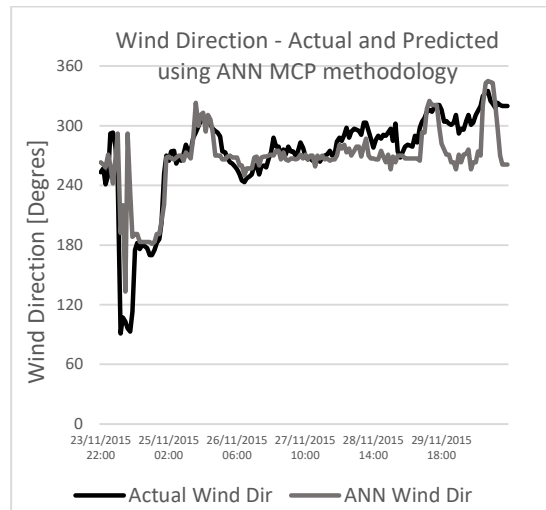
366 **6.1.2 Wind direction with MCP methodology.**

367 Figure 14 to Figure 17 show the wind direction from the period 23rd November to the 30th November
 368 2015. As above, the actual wind direction at the candidate site is compared to that predicted by the
 369 MLR, ANN, DT and SVR methodologies. Again, as in the case for wind speed, there is a similarity
 370 between the actual and predicted wind direction values, in all cases.

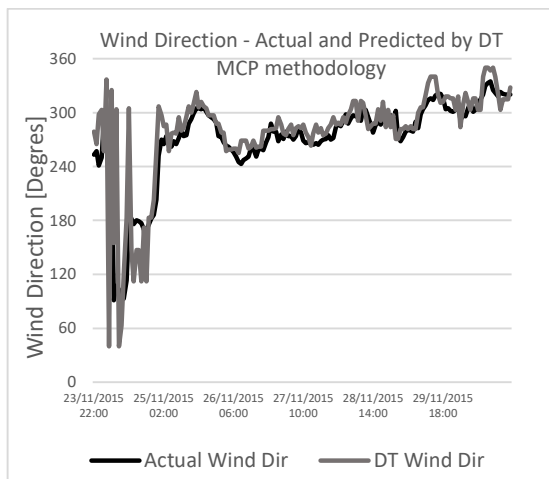
371



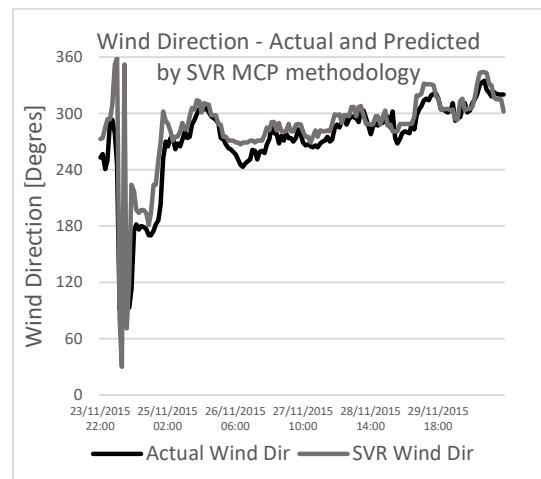
372
373
374
377
Figure 14: Comparing actual and predicted wind direction predicted by MLR methodology, with wind data for 2015



376
378
Figure 15: Comparing actual and predicted wind direction predicted by ANN methodology, with wind data for 2015.



379
380
381
382
383
384
Figure 16: Comparing actual and predicted wind direction predicted by DT methodology, with wind data for 2015

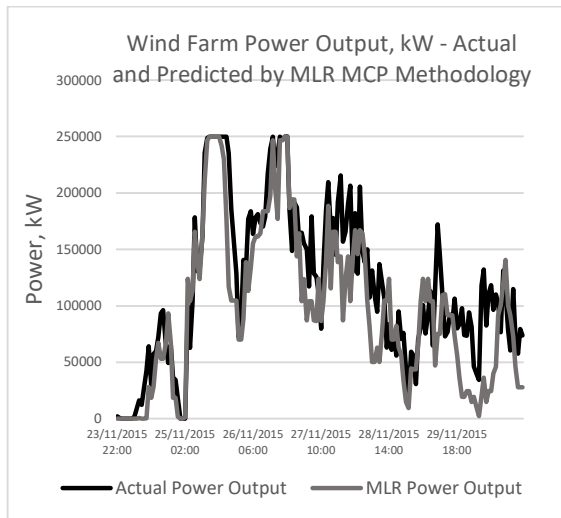


385
386
Figure 17: Comparing actual and predicted wind direction predicted by SVR methodology, with wind data for 2015.

6.2 Wind farm power output with MCP methodology, for a windfarm capacity of 250MW.

387 Figure 18 to Figure 21 compare the output power from the wind farm, which is derived from the actual
388 wind speed and wind direction to the power output derived from the predicted wind speed and direction.
389 This comparison is carried out for the MLR, ANN, DT and SVR methodologies. The results for a wind
390 farm capacity of 250MW are being shown. As in the case for wind speed and direction, the predicted
391 power output closely follows that obtained with the actual wind speed and direction.

392



393
394
395
396
Figure 18: Comparing actual and predicted power output from the wind farm, with wind data for 2015, actual and predicted by MLR methodology. 400

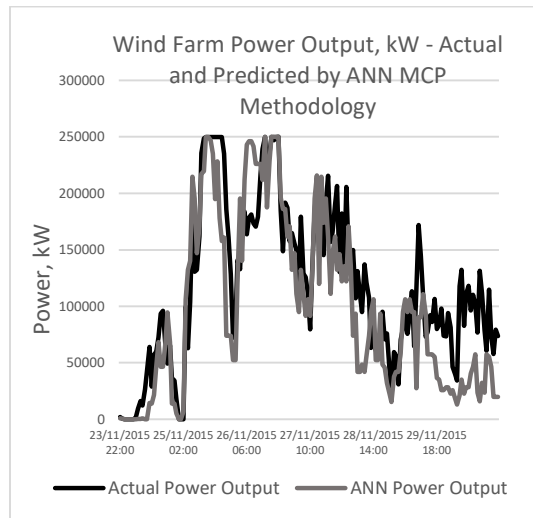
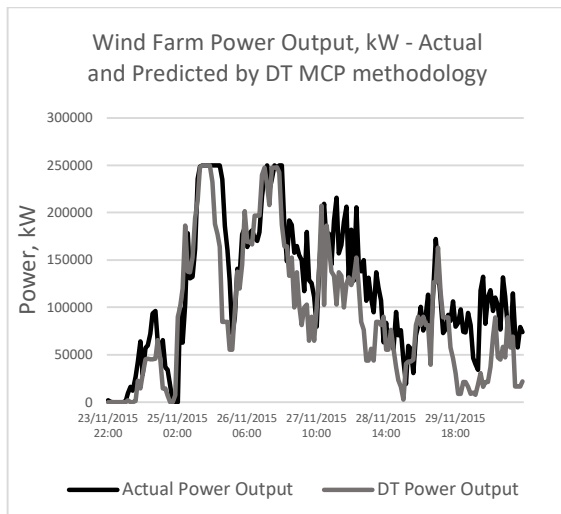


Figure 19: Comparing actual and predicted power output from the wind farm, with wind data for 2015, actual and predicted by ANN methodology. 400



401
402
403
404
Figure 20: Comparing actual and predicted power output from the wind farm, with wind data for 2015, actual and predicted by DT methodology. 408

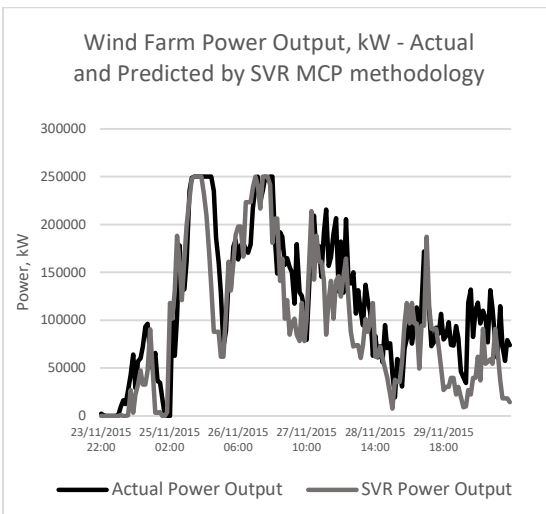


Figure 21: Comparing actual and predicted power output from the wind farm, with wind data for 2015, actual and that predicted by SVR methodology. 408

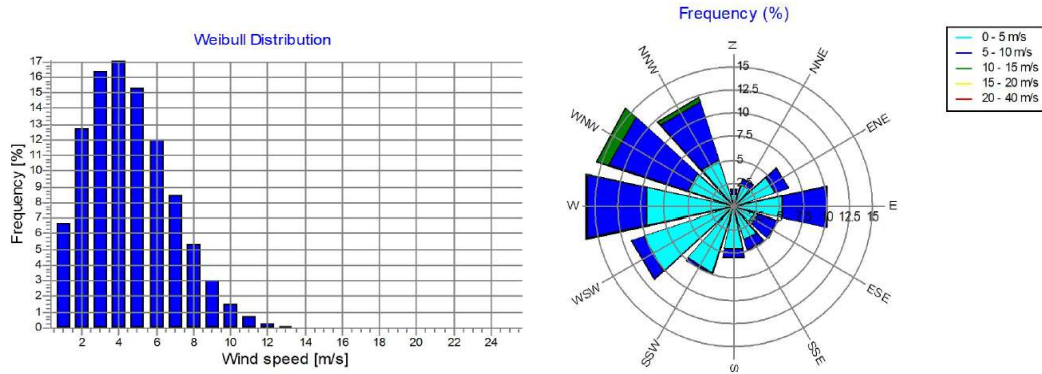
409

410 A Wind Data Analysis, carried out using windPRO®, is shown in the next section. The results presented
411 are a Weibull distribution for wind speed and the wind rose. These charts are computed from the wind
412 speed and direction which are predicted by using the MLR, ANN, DT and SVR MCP methodologies.
413 Thus, the predicted wind speed and direction are compared with the results computed from the actual
414 wind data.

415 6.3 The Actual Wind Data for 2015 measured by the LiDAR system.

416 Figure 22 shows the Wind Data Analysis report from windPRO® for the actual LiDAR data measured
417 at the 80m level height (equivalent to a hub height of 100m). The images show the Weibull distribution
418 for the wind speed and the wind rose. The reports are used to compare the properties of the actual wind
419 measurements and the predicted wind speed and direction.

420



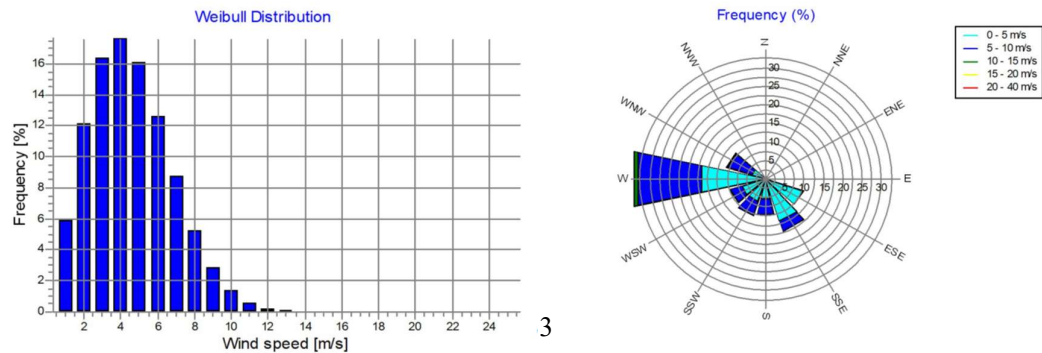
421

422 *Figure 22: windPRO® wind data analysis using actual wind data measured by the LiDAR equipment at a height of 100 m.*

423 **6.4 Wind speed and direction predicted using the MCP methodologies.**

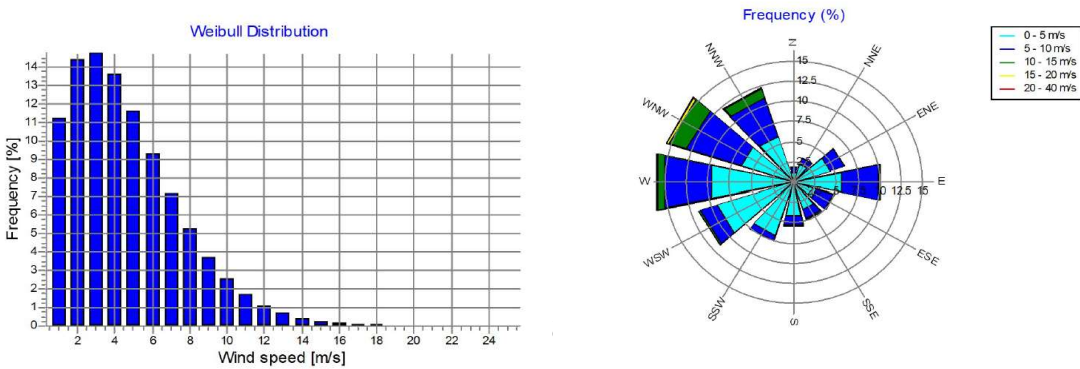
424 Figure 23 to Figure 26 represent the Weibull distribution and the wind rose for the wind speed and
 425 direction predicted by the MLR, ANN, DT and SVR MCP methodologies respectively, at the hub height
 426 of 100m. There exists a similarity between the Weibull plots for the actual wind data and those for the
 427 predicted wind speed, for the same measurement period. While, the wind direction predicted by the
 428 ANN and DT methodologies show a higher resemblance to that of the actual wind direction than that
 429 predicted by the MLR or SVR methodologies. Hence it is expected that the ANN and the DT
 430 methodologies would yield the least error in the predicted power output from the wind farm.

431



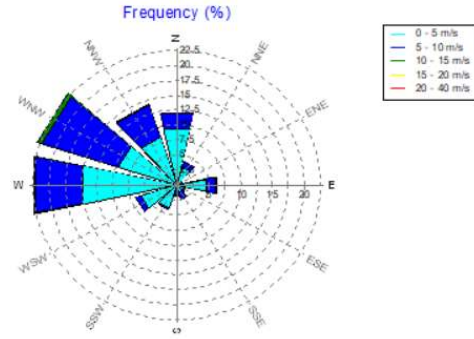
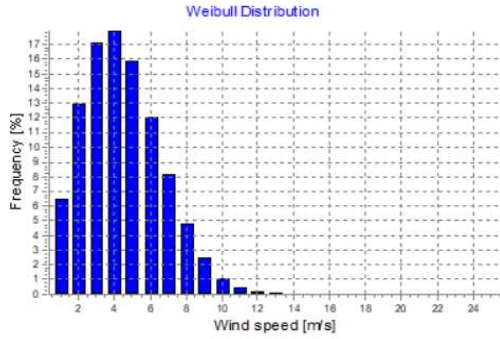
432

434 *Figure 23: windPRO® wind data analysis using wind data predicted by MCP applying MLR at a hub height of 100 m.*



435

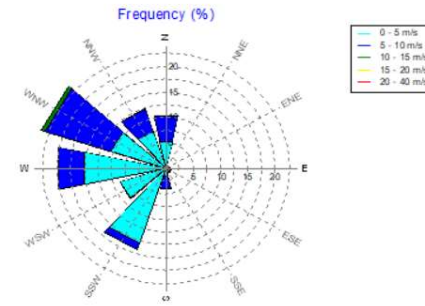
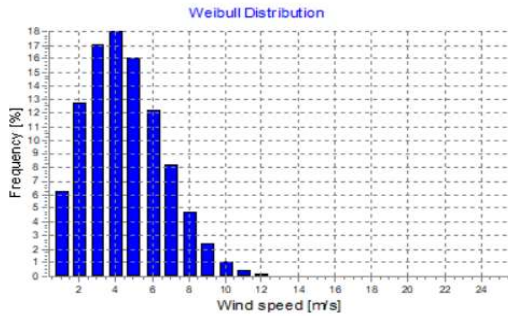
437 *Figure 24: windPRO® wind data analysis using wind data predicted by MCP applying ANN at a hub height of 100 m.*



438

439

440 Figure 25: windPRO® wind data analysis using wind data predicted by MCP applying DT at a hub height of 100 m



441

443 Figure 26: windPRO® wind data analysis using wind data predicted by MCP applying SVR at a hub height of 100 m

444 The results for the NMAE, the NMSE and the percentage error in the overall energy yield are
 445 summarised in Table 6 to Table 8. The tables show that the MLR and ANN methodology have the best
 446 performance in NMAE, NMSE and percentage error in energy yield. The results are consistent for all
 447 wind farm capacities under consideration. ANN is better than MLR in the case of MMAE, while MLR
 448 is slightly better than ANN in the case of the 50MW wind farm capacity. MLR is superior to ANN in
 449 the case of NMSE for all wind farm capacities. However, the differences between the MLR and the
 450 ANN methodologies are minimal and both methodologies show a better performance than the DT or
 451 SVR methodologies. Especially in the case of the overall energy yield as shown in Table 8. Graphical
 452 results are also shown in Figure 27 to Figure 29.

453 Table 6: Summarised results for Normalised Mean Absolute Error (NMAE) by MCP methodology and windfarm capacity.

Normalised Mean Absolute Error				
Wind Farm Capacity	MLR	ANN	DT	SVR
250MW	0.505	0.502	0.572	0.544
200MW	0.502	0.499	0.565	0.539
150MW	0.492	0.482	0.545	0.532
100MW	0.484	0.472	0.537	0.515
50MW	0.510	0.547	0.573	0.558

454 Table 7: Summarised results for the Normalised Mean Squared Error (NMSE) by MCP methodology and windfarm capacity.

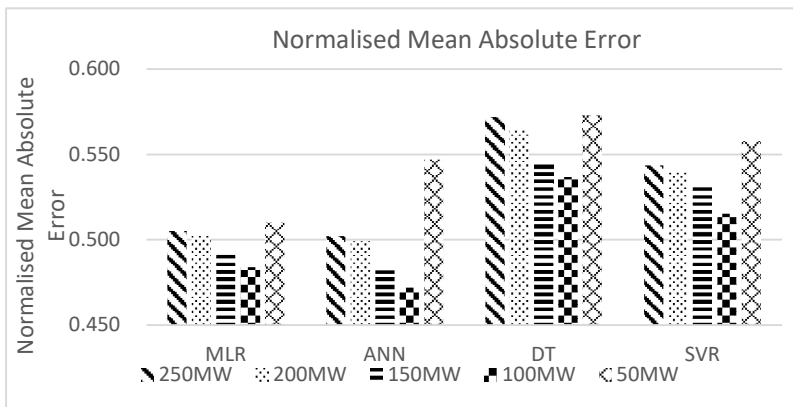
Normalised Mean Squared Error				
-------------------------------	--	--	--	--

<i>Wind Farm Capacity</i>	<i>MLR</i>	<i>ANN</i>	<i>DT</i>	<i>SVR</i>
250MW	0.977	1.004	1.170	1.082
200MW	0.956	0.979	1.123	1.052
150MW	0.912	0.938	1.056	1.002
100MW	0.834	0.868	0.960	0.917
50MW	0.789	0.884	0.930	0.890

455

Table 8: Summarised results for percentage error in overall energy yield by MCP methodology and windfarm capacity.

Percentage Error in Overall Energy Yield				
<i>Wind Farm Capacity</i>	<i>MLR</i>	<i>ANN</i>	<i>DT</i>	<i>SVR</i>
250MW	4.63	4.54	18.83	9.44
200MW	4.80	4.90	18.40	9.34
150MW	4.92	5.40	17.78	9.23
100MW	4.78	5.70	16.92	8.71
50MW	3.65	7.03	14.73	8.23

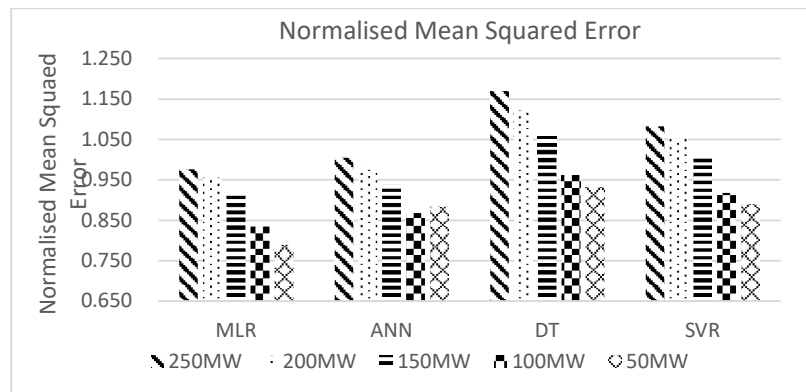


456

457

458

Figure 27: Comparison of the Normalised Mean Absolute Error for the various wind farm topologies and MCP methodology, for the 2015 energy output from the wind farm.

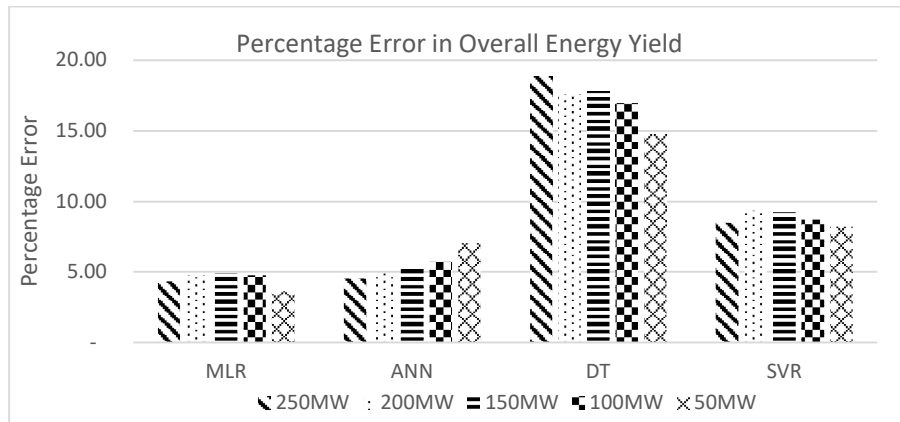


459

460

461

Figure 28: Comparison of the Normalised Mean Squared Error for the various wind farm topologies and MCP methodology, for the 2015 energy output from the wind farm.



462

463 *Figure 29: Comparison of the Percentage Error in Overall Energy Yield for the various wind farm topologies and MCP*
 464 *methodology, for the 2015 energy output from the wind farm.*

465 The ANN methodology also shows the best similarity to the actual wind speed and wind direction, as
 466 seen in Figure 24. In the case of the overall energy yield, the MLR and ANN methodologies show a
 467 significant improvement in percentage error over the DT and SVR methodologies. The ANN
 468 methodology is only better than the MLR methodology for the 250MW windfarm capacity. The MLR
 469 methodology has better results in the case of 200MW, 150MW, 100MW and 50MW wind farm
 470 capacities, with the percentage error being 3.65% at a windfarm capacity of 50MW, when compared to
 471 an error of 7.3% obtained with the ANN methodology.

472 Thus, the metrics show that the best methodologies for predicting the output power from the wind farm
 473 is therefore that which uses the MLR methodology, closely followed by that which uses the ANN
 474 methodology.

475 7. Conclusions

476 The above research has combined the use of MCP methodologies for wind speed and used a different
 477 method for predicting the wind direction at a candidate site. Three of the four MCP methodologies used
 478 are based on modern statistical learning methodologies. The data was collected from a reference site
 479 which is the Island of Malta's international airport, while the candidate site data has been collected by
 480 means of a LiDAR wind measurement system placed on the roof top of a coastal building.

481 The wind direction at the candidate site was predicted with the various MCP methodologies by breaking
 482 down the wind velocity vector into its respective North and East direction components. The regression
 483 analysis was then carried out on the respective components at the reference and the candidate sites. The
 484 wind speed is predicted by using the magnitude of the wind speed at the respective sites for creating the
 485 regression model.

486 The projected wind speed and direction time series were applied to a hypothetical wind farm. Thus, the
 487 error introduced by the four MCP methods could be measured. This was done by calculating the NMAE,
 488 the NMSE and the percentage error in wind farm's energy yield. The results show that the NMAE,
 489 NMSE and the percentage error in energy yield depend on the MCP methodology and the windfarm
 490 capacity, and can be used to establish an optimal MCP methodology.

491 In this case, the best MCP method was that which used MLR. Although other MCP methodologies gave
 492 larger errors, they cannot be totally discarded. It is always best to compare methodologies, comparing
 493 results by analysing residuals and errors and then choosing the best methodology on a case-by-case
 494 basis. In this case the results from the ANN methodology gave results which are very close to the MLR
 495 methodology, while the DT and SV methodologies gave larger errors.

496 Unless actual wind data is available, one cannot carry out this analysis, as the uncertainty is obtained
 497 by comparing the energy from the windfarm with predicted and actual wind data. The above analysis

498 could be done because 18 months of data were available, rather than the normal 12 months, which is
499 usual for a wind resource assessment which uses MCP methodologies.

500 The above study was limited to using the same MCP methodology for both the wind speed and direction
501 and to the N.Ø. Jansen methodology for wake losses. The layout chosen was one that ensured a
502 recommended minimum distance between the wind turbines. Different combinations of MCP
503 methodologies for wind speed and direction can be examined.

504 In this case, an MCP model was created for wind speed, and two more MCP models were created for
505 wind speed components, which were then used to calculate the wind direction. Another possible method
506 is to calculate the magnitude of the wind speed from the models used to calculate the wind direction.
507 This was done, but, the results from the first method, were by far superior to those from the latter
508 method. The reason why, still needs to be investigated as part of future work, and these results are not
509 being presented in this paper. The advantage of having three models, also allows the possibility of using
510 different combinations of MCP methodologies, i.e. using MLR for wind speed and ANN for wind
511 direction. This was also performed for a limited number of combinations and is also the subject of
512 further research

513 Another area which warrants further study, as is trying out different windfarm topologies, or selecting
514 different wind turbines and different hub heights. It would also be of interest to study the application of
515 different wake methodologies as a possible means of decreasing the uncertainties.

516 **8. Author Contribution.**

517 Tonio Sant and Robert. N. Farrugia contributed in the preparation of the manuscript and the research
518 methodology.

519 **9. Competing Interests.**

520 The authors declare that they have no conflict of interest.

521 **10. Acknowledgements.**

522• Mr. Joseph Schiavone from the Meteorological Office at Malta International Airport, Luqa, is being
523 acknowledged for providing the data for the Luqa MIA Weather Station.

524• The authors would like to express their sincere gratitude to Mr. Manuel Aquilina, lab officer at the
525 University of Malta, for technical assistance in collecting and organising the data from the Institute for
526 Sustainable Energy's LiDAR system at Qalet Marku.

527• The LiDAR system was purchased through the European Regional Development Fund (ERDF 335),
528 part-financed by the European Union.

529• Thanks also goes to Din L'Art Helwa for permitting and facilitating the installation of the LiDAR unit
530 on the Qalet Marku Tower.

531• The windPRO® 2.7 software was funded by the project: *Setting up of Mechanical Engineering
532 Computer Modelling and Simulation Laboratory*, part-financed by the European Regional Development
533 Fund (ERDF) - Investing in Competitiveness for a Better Quality of Life, Malta 2007 – 2013.

534 **11. Nomenclature.**

535	ANN	Artificial Neural Network
536	CFD	Computational Fluid Dynamics
537	DT	Decision Trees
538	LiDAR	Light Detection and Ranging
539	LSE	Large Eddy Simulation
540	MCP	Measure-Correlate-Predict
541	MIA	Malta International Airport
542	MLR	Multiple Linear Regression
543	MLP	Multilayer Perceptron

544	MSE	Mean Squared Error
545	NMAE	Normalised Mean Absolute Error
546	NMSE	Normalised Mean Squared Error
547	SLR	Simple Linear Regression
548	SoDAR	Sonic Detection and Ranging
549	SVR	Support Vector Regression
550	WT	Wind Turbine
551	V_i	Magnitude of wind speed in ms^{-1}
552	e_{norm_i}	Normalised residual
553	e_{eng}	Percentage error in energy yield
554	e_i	Residual, MW
555	u_{ip}	Predicted component of wind speed vector in easterly direction at the candidate site in ms^{-1}
556		
557	u_{iref}	Component of wind speed vector in easterly direction at the reference site in ms^{-1}
558		
559	u_{iref}	Component of wind speed vector in easterly direction at the reference site in ms^{-1}
560		
561	u_i	Component of wind speed vector in easterly direction in ms^{-1}
562	v_{ican}	Component of wind speed vector in northerly direction at the candidate site in ms^{-1}
563		
564	v_{ip}	Predicted component of wind speed vector in northerly direction at the candidate site in ms^{-1}
565		
566	v_{iref}	Component of wind speed vector in northerly direction at the reference site in ms^{-1}
567		
568	v_i	Component of wind speed vector in northerly direction in ms^{-1}
569	z_0	surface roughness
570	V_i	Wind speed vector (speed in ms^{-1} , wind direction in deg)
571	$\theta_{math_{ip}}$	Predicted mathematical wind direction at the candidate site in deg
572	$\theta_{met_{ip}}$	Predicted meteorological wind direction at the reference site in deg
573	$\theta_{met_{can}}$	Meteorological wind direction at the candidate site in deg
574	$\theta_{met_{ref}}$	Meteorological wind direction at the reference site in deg
575	θ_{math}	Mathematical wind direction
576	θ_{met}	Meteorological wind direction
577	D	Wind turbine diameter, m
578	N	Number of data points
579	P	Predicted power output from wind farm, MW
580	P_{act}	Actual power output from windfarm, MW
581		

582 **12 References.**

583 Ainslie, J., 1985. Calculating the Flowfield in the Wake of Turbines. *Journal of Wind*
584 *Engineering and Industrial Aerodynamics*, Volume 27, pp. 216 - 224.

585 Alpaydin, E., 2010. *Introduction to Machine Learning*. 2nd Edition ed. s.l.:Massachusetts
586 Institute of Technology.

587 Barthelmie, R. et al., 2006. Comparison of Wake Model Simulations with Offshore Wind
588 Turbine Wake Profiles Measured by Sodar. *Journal of Atmospheric and Oceanic Technology*,
589 Volume 23, pp. 888-901.

590 Bechrakis, D., Deane, J. & MCKeogh, E., 2004. Wind Resource Assessment of an Area using
591 Short-Term Data Correlated to a Long-Term Data-Set.. *Solar Energy*, Volume 76, pp. 724-32.

592 Bilgili, M., Sahin, B. & Yaser, A., 2009. Application of Artificial Neural Networks for the
593 Wind Speed Prediction of Target Station using Reference Stations Data. *Renewable Energy*,
594 Volume 34, pp. 845 - 848.

595 Bilgili, M., Sahlin, B. & Yasar, A., 2007. Application of Artificial Neural Networks for the
596 Wind Speed Prediction of Target Station Using Artificial Intelligent Methods. *Renewable*
597 *Energy*, Volume 32, pp. 2350-60.

598 Bosart, L. & Papin, P., 2017. www.atmos.albany.edu. [Online]
599 Available at: www.atmos.albany.edu/.../2017/pptx/ATM305_Statistics_16Nov17.pptx
600 [Accessed 3 March 2019].

601 Bossanyi, E. et al., 1980. *The Efficiency of Wind Turbine Clusters*. Lyngby, DK, s.n.

602 Carta, J. & Gonzalez, J., 2001. Self-Sufficient Energy Supply for Isolated Communities: Wind-
603 Diesel Systems in the Canary Islands. *Energy Journal*, Volume 22, pp. 115-45.

604 Carta, J. & Velazquez, S., 2011. A New Probabilistic Method to Estimate the Long-Term Wind
605 Speed Characteristics at a Potential Wind Energy Conversion Site. *Energy*, Volume 36, pp.
606 2671-85.

607 Carta, J., Velazquez, S. & Cabrera, P., 2013. A Review of Measure-Correlate-Predict (MCP)
608 methods used to Estimate Long-Term Wind Characteristics at a Target Site. *Renewable and*
609 *Sustainable Energy Reviews*, Volume 27, pp. 362-400.

610 Carta, J., Velazquez, S. & Matias, J., 2011. Use of Bayesian Network Classifiers for Long-
611 Term Mean Wind-Turbine Energy Output Estimation at a Potential Wind Energy Conversion
612 Site. *Energy Conversion and Management*, Volume 52, pp. 1137-49.

613 Churchfield, M., 2013. *A review of Wind Turbine Wake Models and Future Directions*, Boulder,
614 Colorado: National Renewable Energy Laboairy.

615 Clive, J., 2004. Non-linearity of MCP with Weibull Distributed Wind Speeds. *Wind*
616 *Engineering*, Volume 28, pp. 213-24.

617 Cordina, C., Farrugia, R. & Sant, T., 2017. *Wind Profiling using LiDAR at a Costal Location*
618 *on the Mediterranean Island of Malta*. s.l., s.n.

619 Crespo, A. & Hernandez, J., 1986. *A Numerical Model of Wind Turbine Wakes and Wind*
620 *Farms*. Rome, s.n.

621 Crespo, A. & Hernandez, J., 1993. *Analytical Corelations for Turbulence Characteristics in*
622 *the Wakes of Wind Turbines*. Lubeck, s.n.

623 Diaz, S., Carta, J. & Matias, J., 2017. Comparison of Several Measure-Correlate-Predict
624 Models using Support Vector Regression Techniques to estimate wind power densities. A case
625 study. *Energy Conversion and Management*, Volume 140, pp. 334-354.

626 Diaz, S., Carta, J. & Matias, J., 2018. Performance Assessment of Five MCP Models Proposed
627 for the Estimation of Long-term Wind Turbine Power Outputs at a Target Site Using Three
628 Machine Learning Techniques. *Applied Energy*, Issue 209, pp. 455-477.

629 Draper, N. & Smith, H., 2015. *Applied Regression Analysis*. 3rd ed. s.l.:John Wiley and Sons,
630 Inc.

- 631 Fransden, S., 2005. *Turbulence and Turbulence-Generated Structural Loading in Wind Turbine*
632 *Clusters*, s.l.: Riso National Laboratory.
- 633 Gonzales-Longatt, F., Wall, P. & Tezija, V., 2012. Wake Effect in Farm Performance: Steady-
634 State and Dynamic Behaviour. *Renewable Energy*, Volume 39, pp. 329-338.
- 635 Gonzalez-Longatt, F., Wall, P. & Terzija, V., 2012. Wake effect in wind farm performance:
636 Steady State and Dynamic Behaviour. *Renewable Energy*, Volume 39, pp. 329 - 338.
- 637 Google, 2019. *Google Earth*. [Online].
- 638 Hastie, T., Tibshirani, R. & Friedman, J., 2009. *The Elements of Statistical Learning, Data*
639 *Mining, Inference and Prediction*. Second ed. New York: Springer Series in Statistics.
- 640 <https://www.zxlidars.com/wind-lidars/zx-300/>, n.d. [Online]
641 [Accessed 19 January 2020].
- 642 Hu, J., Wang, J. & Zeng, G., 2013. A Hybrid Forecasting Approach Applied to Wind Speed
643 Time Series. *Renewable Energy*, Volume 60, pp. 185 - 194.
- 644 James, G., Witten, D., Hastie, T. & Tibshirane, R., 2015. *An Introduction to Statistical*
645 *Learning with Applications in R*. New York: Springer Texts in Statistics.
- 646 Jensen, N., 1983. *A note on Wind Generator Interaction*, s.l.: Riso National Laboratory.
- 647 Koch, F. et al., 2005. *Consideration of Wind Farm Wake Effect in Power System Dynamic*
648 *Simulation*. s.l., IEEE.
- 649 Lackner, M., A.L., R. & Manwell, J., 2012. *Uncertainty Analysis in Wind resource Assessment*
650 *and Wind Energy Production Estimation*. Reno, Nevada, American Institute of Aeronautics and
651 Astronautics, Inc..
- 652 Larsen, G., Madsen, H. A., Larsen, T. J. & Troldborg, N., 2008. *Wake Modelling and*
653 *Simulation*, s.l.: Technical University of Denmark.
- 654 Larsen, T., Madsen, H., G.C., L. & Hansen, K., 2013. Validation of the Dynamic Wake
655 Meander Model for Loads and Power Production in the Egmond aan Zee Wind Farm. *Wind*
656 *Energy*, 10 October, Volume 16, pp. 605-624.
- 657 Lissaman, P. & Bates, E., 1977. *Energy Effectiveness of Arrays of Wind Energy Conversion*
658 *Systems*, Pasadena, CA: s.n.
- 659 Manwell, J., McGowan, J. & Rogers, A., 2009. *Wind Energy Explained*. 2nd ed. s.l.: John Wiley
660 and Sons Ltd..
- 661 Martin, G., 2011. Underground Pumped Hydroelectric Energy Storage. In: F. Barnes & J.
662 Levine, eds. *Large Energy Storage Systems Handbook*. Boca Raton(Florida): Taylor and
663 Francis Group, pp. 77-109.
- 664 Marvin, L., n.d. *Neural Networks with Matlab*. s.l.: Amazon.
- 665 Mifsud, M., Sant, T. & Farrugia, R., 2018. A Comparison of Measure-Correlate-Predict
666 Methodologies using LiDAR as a Candidate Measurement Device for the Mediterranean Island
667 of Malta. *Renewable Energy*, Issue 127, pp. 947 - 959.
- 668 Monfared, M., Rastegar, H. & Kojabadi, H., 2009. A New Strategy for Wind Speed Forecasting
669 Using Artificial Intelligent Methods. *Renewable Energy*, Volume 34, pp. 845-8.
- 670 Montgomery, D., Peck, E. & Vinning, G., 2006. *Introduction to Linear Regression Analysis*.
671 s.l.: John Wiley & Sons, Inc..

- 672 Oztopal, A., 2006. Artificial Neural Network Approach to Spatial Estimation of Wind Velocity.
673 *Energy Conversion and Management*, Volume 47, pp. 395 - 406.
- 674 Patane, D. et al., 2011. *Long Term Wind Resource Assessment by means of Multivariate Cross-*
675 *Correlation Analysis*. Brussels, Belgium, s.n.
- 676 Perea, A., Amezcua, J. & Probst, O., 2011. Validation of Three New Measure-Correlate
677 Predict Models for the Long-Term Prospection of the Wind Resource. *Journal of Renewable*
678 *and Sustainable Energy*, Volume 3, pp. 1-20.
- 679 Principe, J., Euliano, N. & Curt Lefebvre, W., 2000. *Neural and Adaptive Systems:*
680 *Fundamentals Through Simulations*. s.l.:John Wiley & Sons, Inc..
- 681 Probst, O. & Cardenas, D., 2010. State of the Art and Trends in Wind Resource Assessment.
682 *Energies*, Volume 3, pp. 1087 - 1141.
- 683 Rogers, A., Rogers, J. & Manwell, J., 2005b. Uncertainties in Results of Measure-Correlate-
684 Predict Analyses. *American Wind Energy Association*, May.
- 685 Rogers, A., Rogers, J. & Manwell, J., 2005. Comparison of the Performance of four Measure-
686 Correlate-Predict Models for Long-Term Prospection of the Wind Resource. *Journal of Wind*
687 *Engineering and Industrial Aerodynamics*, 93(3), pp. 243-64.
- 688 Sanderse, B., n.d. *Aerodynamics of wind turbine wakes: Literature review*, s.l.: Energy
689 Research Centre of the Netherlands.
- 690 Santamaria-Bonfil, G., Reyes-Ballestros, A. & Gershenson, C., 2016. Wind Speed Forecasting
691 for Wind Farms: A Method Based on Support Vector Regression. *Renewable Energy*, Volume
692 85, pp. 790-809.
- 693 Scholkopf, B. & Smola, A., 2002. *Learning with Kernels - Support Vector Machines,*
694 *Regularisation, Optimisation and Beyond*. Cambridge(Massachusetts): The MIT Press.
- 695 Scott, I. & Lee, S.-L., 2011. Battery Energy Storage. In: F. Barnes & J. Levine, eds. *Large*
696 *Energy Storage Systems Handbook*. Boca Raton(Florida): Taylor and Francis Group, pp. 153-
697 197.
- 698 Shcherbakov, M. et al., 2013. A survey of Forecast Error Measures. *World Applied Sciences*
699 *Journal*, Volume 24, pp. 171 - 176.
- 700 Vapnik, V., 1995. *The Nature of Statistical Learning Theory*. NY: Springer.
- 701 Vapnik, V., Golowich, S. & Smola, A., 1998. A Support Vector Method for Function
702 Approximation, Regression Estimation and Signal Processing. *Advances in Neural Information*
703 *Processing Systems*, pp. 281-7.
- 704 Velazquez, S., Carta, J. & Matias, J., 2011. Comparison between ANNs and Linear MCP
705 algorithms in the Long-Term Estimation of the Cost per kW h Produced by a Wind Turbine
706 at a Candidate Site: A Case Study in the Canary Islands. *Applied Energy*, Volume 88, pp. 3869-
707 81.
- 708 Vermeulen, P., 1980. *An Experimental Analysis of Wind Turbine Wakes*. Lyngby, DK, s.n., pp.
709 431-450.
- 710 Vermeulen, P., Builtjes, P., Dekker, J. & Lammerts van Buren, G., 1979. *An Experimental*
711 *Study of the Wake Behind a Full-Scale Vertical-Axis Wind Turbine*, s.l.: s.n.

712 wind-turbine-models.com, 2019. *wind-turbine-models.com*. [Online]
713 Available at: <https://en.wind-turbine-models.com/turbines/1-repower-5m-offshore>
714 [Accessed 19 March 2019].

715 Zhang, J., Chowdhury, S., Messac, A. & Hodge, B.-M., 2014. A Hybrid Measure-Correlate-
716 Predict Method for Long-Term Wind Condition Assessment. *Energy Conversion and*
717 *Management*, Volume 87, pp. 697-710.

718 Zhao, P., Xia, J., Dai, Y. & He, J., 2010. *Wind Speed Prediction Using Support Vector*
719 *Regression*. Taiwan, IEEE.

720

721